

The Effect of the Lanthanoid Contraction on the Nonaaqualanthanoid(III) Tris(trifluoromethanesulfonates)

BY A. CHATTERJEE, E. N. MASLEN AND K. J. WATSON

Department of Physics, University of Western Australia, Nedlands, Australia 6009

(Received 12 May 1986; accepted 12 February 1988)

Abstract

The $[\text{Ln}(\text{H}_2\text{O})_9](\text{CF}_3\text{SO}_3)_3$ complexes with Ln = La, Ce, Pr, Nd, Sm, Eu, Gd, Tb, Dy, Yb and Lu form an isomorphous series of hexagonal structures, $a = 13.990$ (6)– 13.259 (2), $c = 7.444$ (2)– 7.751 (1) Å, $P6_3/m$, $Z = 2$. Full crystal data have been published [Harrowfield, Kepert, Patrick & White (1983). *Aust. J. Chem.* **36**, 483–492]. The $[\text{Ln}(\text{H}_2\text{O})_9]^{3+}$ moiety has a tricapped trigonal prism geometry. The consequences of the lanthanoid contraction were determined from structure refinements with X-ray diffraction intensity data measured for a charge density study at 295 K ($wR = 0.022$ – 0.051). The Nd structure was also refined with neutron diffraction data ($wR = 0.042$). The lanthanoid contraction for the bonds to the equatorial oxygens is less than it is for the prism oxygens. This is associated with weakening of the hydrogen-bond network for the equatorial water, while that of the prism water is strengthened. This reflects a change in the interaction between the metal and the ligating water molecules resulting from their orientation. At the upper end of the $4f$ series, the trigonally oriented water is less strongly bound.

Introduction

Single crystals of nona-aqualanthanoid(III) tris(trifluoromethanesulfonates), known as lanthanoid triflates, form an isomorphous series for which some structures were determined by Harrowfield, Kepert, Patrick & White (1983). The quality of the data for those studies indicated that the structures would be suitable for more detailed study, including analysis of the electron-density distribution. Structures for the neodymium and holmium members of the series have been determined more recently by Paiva Santos, Castellano, Machado & Vicentini (1985).

Each lanthanoid atom lies on a $\bar{6}$ site, and is coordinated to the O atoms of nine water molecules situated at the vertices of a tricapped trigonal prism, the hydrated complex cation thereby having $\bar{6}$ symmetry.

The water molecules at the equatorial positions are oriented with the H atoms above and below the mirror plane, each bonding to a trifluoromethanesulfonate group. The geometry at the O atom for these hydrogen

bonds and the oxygen–metal bond is approximately trigonal. The hydrogens of the prism water molecules are also involved in hydrogen bonds, but their orientation relative to the corresponding oxygen–metal bond is asymmetrical, the geometry at the oxygen being closer to tetrahedral than trigonal.

Data collection

Single crystals were kindly supplied by Drs J. M. Patrick and J. M. Harrowfield. Unit-cell dimensions for each complex, except that of promethium, were determined by least-squares methods from the optimized Bragg angles of approximately twelve reflections, consisting of Friedel pairs of axial reflections and some others in the range $20 < 2\theta < 30^\circ$. The results were consistent with those recorded by Harrowfield *et al.* (1983), which were preferred for all further work. Consequently the new values are not recorded here.

Intensity data for the La, Ce, Pr, Nd, Sm, Eu, Gd, Tb, Dy, Yb and Lu members of the series were carefully measured using a θ – 2θ step-scan procedure on a Syntex $P2_1$ four-circle diffractometer, with graphite-monochromatized Mo $K\alpha$ radiation ($\lambda = 0.71069$ Å). The crystals used in the data collection were fairly regular hexagonal prisms. The quality of each crystal was checked carefully before intensity measurements by sampling reflection profiles and comparing intensities for a representative selection of Friedel pairs. Table 1(a) gives numerical details for each experiment. The indices for the measured reflections range from -23 to 23 for h and k and from 0 to 14 for l .

For each crystal the intensities of the six standard reflections equivalent to one $h00$ and the two equivalent to one $00l$ reflection were measured regularly. Typically the standards varied by $\pm 5\%$ during the experiment. The major part of this variation was consistent with slow fluctuation of the primary beam intensity. The crystals of the heavier members of the series tended to deteriorate owing to loss of water. These were coated with araldite which, with some exceptions, was successful in controlling the degradation.

The intensities of symmetry-related reflections were monitored carefully. For the cerium, neodymium and

Table 1. X-ray data collection and refinement indices for rare-earth metal triflates

(a) Data collection									
	Crystal dimensions (mm)				No. of reflections		$(\sin\theta/\lambda)_{\max}$ (\AA^{-1})	μ (mm^{-1})	R_{int}
	[100]	[010]	[110]	[001]	M	N			
La	0.154	0.098	0.194	0.320	3805	3221	0.95	2.06	0.021
Ce	0.164	0.240	0.260	0.360	7874	3194	0.96	2.22	0.017
Pr	0.156	0.154	0.144	0.336	7595	3185	0.96	2.31	0.020
Nd	0.096	0.098	0.102	0.330	7476	3169	0.95	2.46	0.032
Sm	0.174	0.154	0.194	0.240	7501	3144	0.96	2.76	0.034
Eu	0.112	0.184	0.168	0.360	7533	3139	0.96	2.92	0.036
Gd	0.356	0.176	0.178	0.400	3879	3128	0.95	3.09	0.026
Tb	0.156	0.138	0.143	0.294	6370	2685	0.91	3.30	0.018
Dy	0.196	0.212	0.214	0.400	7338	3093	0.95	3.49	0.018
Yb	0.250	0.434	0.366	0.450	10839	3033	0.95	4.29	0.039
Lu	0.253	0.263	0.260	0.440	6158	2590	0.91	4.58	0.025

M is the number of measured reflections, N is the number of unique reflections, $R_{\text{int}} = \sum |I - \langle I \rangle| / \sum I$ for all repeated reflections.

(b) Refinement indices						
	R	wR	S	$\Delta\rho_{\min}$ (e \AA^{-3})	$\Delta\rho_{\max}$ (e \AA^{-3})	
La	0.063	0.029	2.26	-0.9	1.2	
Ce	0.052	0.033	1.16	-0.6	1.1	
Pr	0.055	0.022	1.71	-1.2	1.2	
Nd	0.061	0.022	1.66	-1.3	1.3	
Sm	0.057	0.026	1.37	-1.5	1.4	
Eu	0.059	0.031	3.08	-0.8	1.2	
Gd	0.059	0.030	1.46	-1.6	1.3	
Tb	0.054	0.024	1.39	-1.6	1.3	
Dy	0.073	0.021	2.70	-1.7	1.2	
Yb	0.053	0.044	1.26	-3.3	4.8	
Lu	0.075	0.051	1.92	-4.3	6.0	

$S = \{\sum w_i [F_o - kF_c]^2 / (N - n_i)\}^{1/2}$, where k is the scale factor and n_i is the number of variables. $\Delta\rho_{\min}$ is at the centre of the metal atom for the La, Ce, Pr, Nd, Sm, Eu, Gd, Tb and Dy structures, and 0.5 Å from the metal along Ln—O(1) for the Yb and Lu structures; $\Delta\rho_{\max}$ is 0.5 Å from the metal centre, opposite the Ln—O(1) bond.

dysprosium compounds data collection was repeated with several crystals before satisfactory internal consistency was achieved.

The data were rescaled following the variation in intensity of the standard reflections. The maximum rescaling factor among the accepted data sets was 1.05. Lorentz and polarization corrections were applied. Absorption corrections were evaluated by the analytical method described by de Meulenaer & Tompa (1965). The maximum and minimum transmission factors differed by up to 15%, the range for one of the more strongly absorbing samples being 0.36 to 0.40. The internal consistency factors are included in Table 1(a).

Unless there were large discrepancies from known causes all equivalent intensities were averaged. The variances for the averaged reflection intensities were derived initially from counting statistics. These were adjusted to allow for fluctuations in the primary beam intensity determined from the standard reflections, using a version of the *DATCO5* program in the *XRAY76* system (Stewart, 1976). The variances were then further modified as indicated by comparison of equivalent reflections using the procedure of Elcombe, Cox, Pryor & Moore (1971). Structure amplitudes were adjusted to correct for negative intensities by the Bayesian statistics method of French & Wilson (1978).

Neutron experiment

In order to obtain reliable parameters for the H atoms, neutron diffraction data were measured for the neo-

dymium member of the series using the four-circle diffractometer on the 2-Tan B neutron beam from the HIFAR reactor at the Australian Atomic Energy Commission Research Establishment at Lucas Heights, New South Wales. The incident unpolarized, graphite-monochromatized beam wavelength was 1.237 Å, and flux at the sample position was 8×10^3 neutrons $\text{mm}^{-2} \text{s}^{-1}$. The crystal was a hexagonal prism with one pair of faces suppressed, with dimensions $4.0 \times 3.75 \times 1.8$ mm.

Integrated intensities for all reflections with $\sin\theta/\lambda < 0.53 \text{ \AA}^{-1}$ were measured using a θ - 2θ step-scan at a rate of $0.3^\circ \text{ min}^{-1}$. Total 2θ scan interval 3.0° for $2\theta < 45^\circ$ and 4.5° for $45 < 2\theta < 81.2^\circ$. One standard (550) measured every 25 reflections. 2396 measured intensities reduced to 424 unique reflections following the procedure described above for the X-ray data. The equivalent indices range from -12 to 12 for h and k , and 0 to 7 for l , with $\sin\theta/\lambda$ from 0.042 to 0.526 \AA^{-1} .

The linear absorption coefficient, $\mu = 0.121 \text{ mm}^{-1}$, was computed from neodymium absorption and incoherent cross sections (Moore, 1981), from the value for F, O, S and C using the ν^{-1} law (Bacon, 1975, ch. 2) and from the mean absorption correction for the chemically bonded H atom of 39.4 b (Melkonian, 1949). The transmission factors ranged from 0.59 to 0.73.

Refinements

X-ray structure factors were evaluated for each member of the series using the bonded atom scattering

Table 2. X-ray positional and thermal parameters of the lanthanoid atoms

(a) Fractional atomic coordinates of lanthanoid atoms ($\frac{2}{3}, \frac{1}{3}, \frac{1}{2}$)(b) Thermal parameters ($\text{\AA}^2 \times 10^3$). The anisotropic temperature factor is of the form $\exp[-2\pi^2(U_{11}h^2a^{*2} + \dots + 2U_{13}hla^*c^*)]$. $U_{13} = U_{23} = 0$. E.s.d.'s refer to the least significant digits.

	$U_{11} = U_{22}$	U_{33}	$U_{12} = (U_{11})/2$
La	2.865 (6)	2.682 (11)	1.433 (4)
Ce	2.716 (5)	2.558 (10)	1.358 (3)
Pr	2.756 (5)	2.557 (9)	1.378 (3)
Nd	2.695 (5)	2.670 (9)	1.348 (3)
Sm	2.715 (5)	2.642 (8)	1.357 (3)
Eu	2.755 (6)	2.637 (10)	1.378 (4)
Gd	2.841 (6)	2.574 (9)	1.421 (4)
Tb	2.747 (6)	2.596 (9)	1.373 (4)
Dy	2.876 (6)	2.618 (10)	1.438 (4)
Yb	3.784 (6)	2.416 (9)	1.892 (4)
Lu	4.415 (12)	2.461 (15)	2.208 (8)

factor pf (Stewart, Davidson & Simpson, 1965) for hydrogen and the relativistic Hartree-Fock scattering factors with $\Delta f'$ and $\Delta f''$ from *International Tables for X-ray Crystallography* (1974) for Ln, C, F, O and S. Assuming anisotropic thermal motion for all atoms except hydrogens, the structural parameters and the scale factor were refined by full-matrix least-squares methods. The residual minimized was based on $|F|$. The weight for each reflection was the reciprocal of the variance. Refinement in each case was continued until all parameter shifts were less than 0.05σ for non-H atoms, and 0.1σ for H. An isotropic extinction parameter was included on a trial basis in the later stage of each refinement. The corrections applied were for secondary extinction as described by Larson (1970). The values of r^* obtained were insignificant in terms of the standard deviation and randomly positive or negative. This indicated negligible extinction for all structures. Reliability indices for the refinements are included in Table 1(b).

The atomic parameters agree with those reported by Paiva Santos *et al.* (1985) for the neodymium complex at tolerances consistent with the standard deviations. The results reported here are more precise, as expected, because of the larger data set. The hydrogen parameters agree less well, suggesting that these are affected by the difference in resolution of the two experiments.

The neutron structure for the neodymium complex was determined in a similar manner, except that anisotropic thermal parameters were varied for all atoms. The neutron scattering lengths of 7.5, 2.8, 5.6, 5.8, 6.6 and -0.37 fm for Nd, S, F, O, C and H respectively were as listed by Bacon (1975). Refinement was continued until all shifts were less than 0.05σ , at which stage the refinement indices R and wR were 0.042 and 0.042 respectively. The neutron results are far more precise for the H atoms, but are less accurate for C, F, Nd, O and S because of the limited range of the neutron data. There was again no evidence for extinction in the F_o versus F_c agreement, as a trial refinement of extinction using the procedure of Larson (1970) gave an insignificant value for r^* .

The X-ray coordinates and thermal parameters for all the metal atoms are given in Table 2. Table 3 lists the atomic parameters obtained from the X-ray and neutron refinements of neodymium triflate. The X-ray and neutron coordinates for all non-H atoms coincide quite closely. The agreement between the thermal parameters is less satisfactory, the neutron U_{33} values being consistently lower than the X-ray values.

Relevant bond lengths, angles and interatomic distances from the analyses are given in Tables 4 and 5 respectively.*

Discussion

The variation of the unit-cell dimensions for the lanthanum to lutetium crystals determined by Harrowfield *et al.* (1983) is plotted in Fig. 1. Whereas a contracts, c expands across the series. In each case, however, there is a discontinuity at the gadolinium member. It seems relevant that the Gd^{3+} ion has an f^7 configuration; that is, its f shell is half-filled. This suggests that the effect of adding an f electron to form a spin pair is quantitatively different from that of adding an electron with a spin that is unpaired.

This result is analogous to those for the corresponding lanthanoid bromates and ethylsulfates (Albertsson & Elding, 1977). All three series of structures are similar, in being hexagonal with the rare-earth atoms at special positions. The ethylsulfates and triflates have the same symmetry, a subgroup of that for the bromates, which have a different hydrogen-bond network. For the bromates the $[\text{Ln}(\text{H}_2\text{O})_9]^{3+}$ ion has $\bar{6}m2$ symmetry, with the H atoms associated with the equatorial oxygens lying in the equatorial plane, and with the orientation of the prism water molecules symmetrical, but not trigonal.

For the ethylsulfates and triflates, in which the cation has $\bar{6}$ symmetry, the equatorial waters have H atoms arranged symmetrically above and below the mirror plane, but the prism waters are unsymmetrical. In view of this it is unlikely that the discontinuity at Gd shown in Fig. 1 is a property of the total structure. It must be characteristic of the $[\text{Ln}(\text{H}_2\text{O})_9]^{3+}$ ion alone.

A projection of the structure for the praseodymium member of the series is shown in Fig. 2. Columns of $[\text{Ln}(\text{H}_2\text{O})_9]^{3+}$ cations centred on the $\bar{6}$ axis at $x = \frac{2}{3}$, $y = \frac{1}{3}$ run parallel to the unique axis, with corresponding columns of $[\text{CF}_3\text{SO}_3]^-$ anions arranged in groups of three about the 6_3 axis through the origin. The respective columns are linked *via* a three-dimensional network of hydrogen bonds. Detailed properties

* Lists of structure factors, atomic coordinates, thermal parameters and unit-cell dimensions for all compounds studied have been deposited with the British Library Document Supply Centre as Supplementary Publication No. SUP 44764 (627 pp.). Copies may be obtained through The Executive Secretary, International Union of Crystallography, 5 Abbey Square, Chester CH1 2HU, England.

Table 3. Fractional atomic coordinates ($\times 10^4$) and thermal parameters ($\text{\AA}^2 \times 10^4$) in neodymium triflate obtained from X-ray and neutron diffraction analyses

Neutron parameters appear under corresponding X-ray values. E.s.d.'s in parentheses refer to the least significant digits.

	<i>x</i>	<i>y</i>	<i>z</i>	<i>U</i> ₁₁	<i>U</i> ₂₂	<i>U</i> ₃₃	<i>U</i> ₁₂	<i>U</i> ₁₃	<i>U</i> ₂₃
Nd	20000/3 20000/3	10000/3 10000/3	2500 2500	269.5 (5) 266 (1)	269.5 (5) 266 (1)	267.0 (9) 174 (2)	134.8 (3) 133 (1)	0 0	0 0
O(1)	4890 (2) 4890 (3)	1409 (2) 1407 (3)	2500 2500	365 (9) 381 (24)	397 (9) 416 (26)	443 (10) 365 (25)	70 (8) 92 (21)	0 0	0 0
O(2)	6646 (1) 6646 (3)	2078 (1) 2061 (3)	166 (2) 164 (4)	458 (7) 444 (19)	421 (21) 421 (21)	438 (7) 344 (14)	154 (5) 184 (17)	127 (6) 100 (13)	-15 (6) -39 (15)
O(3)	175 (1) 174 (2)	6195 (1) 6190 (2)	869 (2) 871 (3)	414 (7) 470 (16)	676 (9) 735 (18)	436 (7) 387 (12)	159 (6) 184 (13)	-39 (6) -36 (11)	-153 (7) -157 (13)
O(4)	1819 (1) 1814 (3)	7501 (2) 7498 (3)	2500 2500	278 (8) 345 (22)	713 (13) 750 (26)	441 (10) 362 (17)	124 (9) 155 (20)	0 0	0 0
H(1)	4494 (16) 4523 (4)	958 (16) 1003 (4)	1410 (30) 1459 (6)	872 (79) 701 (32)	664 (31) 446 (30)	183 (28) 183 (28)	-109 (23) 105 (21)	-45 (24) -21 (26)	
H(2a)	6442 (18) 6372 (4)	1487 (18) 1319 (6)	297 (33) 373 (6)	713 (82) 773 (33)	491 (32) 525 (25)	288 (30) 288 (30)	105 (21) 105 (21)	-21 (26) -21 (26)	
H(2b)	7088 (15) 7222 (4)	2250 (17) 2287 (4)	-602 (26) -732 (6)	589 (69) 600 (28)	619 (29) 467 (3)	428 (22) 332 (3)	243 (24) 137 (2)	145 (25) 0	-2 (21)
S(1)	622 (1) 628 (5)	6810 (1) 6822 (5)	2500 2500	289 (3) 295 (40)	289 (3) 434 (38)	268 (28) 268 (28)	135 (33) 135 (33)	0 0	0 0
C(1)	122 (3) 115 (3)	7804 (3) 7801 (3)	2500 2500	649 (22) 748 (30)	703 (23) 783 (28)	829 (25) 766 (24)	353 (19) 454 (23)	0 0	0 0
F(1)	-975 (2) -988 (4)	7262 (2) 7249 (5)	2500 2500	690 (14) 675 (38)	1276 (20) 1334 (46)	1391 (22) 1221 (43)	661 (15) 675 (35)	0 0	0 0
F(2)	474 (2) 478 (4)	8423 (1) 8437 (4)	1069 (3) 1070 (7)	1432 (16) 1427 (38)	1168 (14) 1219 (35)	1605 (17) 1565 (41)	787 (13) 775 (31)	265 (15) 267 (34)	728 (14) 757 (34)

Table 4. Metal-to-equatorial and -prism oxygen bond lengths (\AA) and angles ($^\circ$)E.s.d.'s in parentheses refer to the least significant digit. O(1) = equatorial oxygen, $d_1 = \text{Ln}-\text{O}(1)$; O(2) = prism oxygen, $d_2 = \text{Ln}-\text{O}(2)$; $r = d_1/d_2$; $\alpha_1 = \text{O}(1)-\text{Ln}-\text{O}(2)$; $\alpha_2 = \text{O}(1)-\text{Ln}-\text{O}(2)^\circ$.

	d_1	d_2	r	α_1	α_2
La	2.611 (2)	2.513 (2)	1.039	65.9 (1)	72.7 (1)
Ce	2.594 (2)	2.489 (2)	1.042	66.1 (1)	72.7 (1)
Pr	2.579 (2)	2.469 (2)	1.045	66.2 (1)	72.6 (1)
Nd	2.571 (2)	2.451 (2)	1.049	66.3 (1)	72.6 (1)
Nd*	2.572 (2)	2.469 (2)	1.042	66.1 (1)	72.5 (1)
Sm	2.548 (2)	2.418 (2)	1.054	66.4 (1)	72.4 (1)
Eu	2.536 (2)	2.408 (2)	1.053	66.5 (1)	72.3 (1)
Gd	2.536 (2)	2.395 (2)	1.059	66.5 (1)	72.3 (1)
Tb	2.527 (2)	2.378 (2)	1.063	66.6 (1)	72.3 (1)
Dy	2.520 (2)	2.363 (2)	1.066	66.6 (1)	72.2 (1)
Yb	2.532 (3)	2.302 (3)	1.100	66.9 (1)	71.4 (1)
Lu	2.519 (5)	2.287 (4)	1.101	67.0 (2)	71.1 (2)

* Neutron data refinement.

of the structures of lanthanum, gadolinium and lutetium triflates are described by Harrowfield *et al.* (1983).Both the metal-prism oxygen [$\text{Ln}-\text{O}(2)$] and the metal-equatorial oxygen [$\text{Ln}-\text{O}(1)$] bond lengths decrease monotonically through the series lanthanum to lutetium. The rate of decrease is larger for the $\text{Ln}-\text{O}(2)$ bond, which is shorter in all cases. Although the metal-prism oxygen bond lengths decrease monotonically, the rate declines as the number of 4f electrons increases.Harrowfield *et al.* (1983) attributed this differential contraction to an increasing tendency for the metal ion to change coordination number from nine to six as its size is reduced, but did not attempt to explain the differential effect for the equatorial oxygens in detail. Their arguments are supported by Spedding, Pikal & Ayres (1966), but other authors (Reuben & Fiat, 1969; Geier, Karlen & Zelewsky 1969; Geier & Karlen,Table 5. Interatomic distances (\AA) in lanthanoid triflates

E.s.d.'s in parentheses refer to the least significant digit.

The superscripts refer to the following equivalent sites: (i) $1+y-x, 1-x, z$; (ii) $1-y, x-y, z$; (iii) $x, y, \frac{1}{2}-z$; (iv) $1-y, x-y, \frac{1}{2}-z$; (v) $1+y-x, 1-x, \frac{1}{2}-z$; (vi) $y-x, -x, z$; (vii) $1-x, 1-y, -z$; (viii) $1-(y-x), x, -z$; (ix) $y, y-x, -z$. $A = \text{O}(1)-\text{O}(2)$, $B = \text{O}(1)-\text{O}(2^i)$, $C = \text{O}(1)-\text{O}(3^{\text{viii}})$, $D = \text{O}(2)-\dots$
 $\text{O}(4^{\text{vii}})$, $E = \text{O}(2)-\text{O}(2^{\text{iii}})$, $F = \text{O}(2)-\text{O}(2^{\text{ii}})$, $G = \text{O}(2)-\text{O}(3^{\text{vi}})$.

	<i>A</i>	<i>B</i>	<i>C</i>	<i>D</i>	<i>E</i>	<i>F</i>	<i>G</i>
LATFS	2.788 (3)	3.039 (3)	2.932 (2)	2.753 (2)	3.550 (3)	3.080 (4)	2.843 (3)
CETFS	2.773 (3)	3.014 (3)	2.934 (2)	2.756 (3)	3.528 (3)	3.042 (3)	2.838 (3)
PRTFS	2.759 (2)	2.990 (3)	2.947 (2)	2.752 (2)	3.504 (2)	3.014 (3)	2.839 (2)
NDTFS	2.749 (2)	2.973 (2)	2.945 (2)	2.754 (2)	3.482 (2)	2.989 (3)	2.841 (2)
NDTFS*	2.752 (2)	2.981 (2)	2.945 (2)	2.752 (2)	3.485 (2)	3.030 (3)	2.816 (2)
SMTFS	2.722 (2)	2.936 (3)	2.953 (2)	2.755 (2)	3.433 (3)	2.951 (3)	2.831 (3)
EUTFS	2.713 (3)	2.922 (3)	2.965 (2)	2.750 (2)	3.424 (3)	2.932 (4)	2.827 (3)
GDTFS	2.707 (2)	2.912 (2)	2.966 (2)	2.750 (2)	3.402 (2)	2.921 (3)	2.825 (3)
TBTFS	2.695 (2)	2.895 (3)	2.978 (2)	2.747 (2)	3.379 (2)	2.900 (3)	2.823 (3)
DYTF	2.684 (2)	2.879 (3)	2.987 (2)	2.751 (2)	3.351 (2)	2.886 (3)	2.823 (3)
YBTFS	2.671 (4)	2.828 (4)	3.002 (3)	2.739 (3)	3.231 (3)	2.840 (5)	2.804 (4)
LUTFS	2.660 (7)	2.801 (7)	3.012 (4)	2.739 (5)	3.193 (5)	2.837 (9)	2.797 (6)

* Neutron data refinement.

1971) argue in favour of constant coordination number along the rare-earth series.

Similar differences in the rates of contraction for the bonds to equatorial and prism oxygens for the bromates and ethylsulfates reported by Albertsson & Elding (1977) are ascribed by them to the effect of steric repulsion between the equatorial and prism oxygens. If that explanation were correct, a marked change in the asymmetry of the $[\text{Ln}(\text{H}_2\text{O})_9]^{3+}$ ion would be expected as the steric interaction increased; that is, the geometry for $[\text{Lu}(\text{H}_2\text{O})_9]^{3+}$ would be closer to $\bar{6}m2$ symmetry than that for $[\text{Ce}(\text{H}_2\text{O})_9]^{3+}$. This is not observed. It is also difficult to explain the differential contraction mechanistically with mutual repulsion of the oxygens as the sole cause.

For neodymium triflate the water O—H distances are longer in the neutron analysis. This is the well known bias of the positions due to the valence-electron distribution in X-ray structure refinements. Otherwise the neutron diffraction analysis confirms the locations of the H atoms assigned in the X-ray experiments. The geometry indicates these to be reliable for all members except the lutetium structure where the H atoms

attached to O(1) have large thermal motion [$U = 0.112(28) \text{ \AA}^2$]. The corresponding neutron and X-ray parameters for the equatorial oxygens agree within one standard deviation, but for the prism oxygen there is a significant difference in the y coordinate, and in some components of the thermal tensor. As a result the metal—prism oxygen bond length is 0.02 \AA longer in the neutron structure. This is consistent with a refinement bias in the X-ray structure analysis associated with displacement of the oxygen positions towards the lone pairs.

In the hydrogen-bond system the equatorial O(1) atom is linked to O(3) atoms in the sulfonate group, while the prism oxygen is linked to O(3) and O(4) in another anion. In progressing through the series from the lanthanum to the lutetium triflates (*i.e.* as the number of $4f$ electrons increases) the length of the hydrogen bond O(1)···O(3^{viii}) increases, that of O(2)···O(3^{vi}) contracts while that of O(2)···O(4^{vii}) is almost unchanged (Table 5).

These trends are accompanied by a change in the packing density, which increases along [001] and decreases in the ab plane. This is reflected in the thermal motion of the atoms. Plots of the U_{11} and U_{33} vibration-tensor elements for the lanthanoid atoms through the series are shown in Fig. 1. The rare-earth U_{11} component and the mean-square amplitude for O(1) increase, while the rare-earth U_{33} component decreases, across the series. In contrast with this, the thermal motion for the sulfonate group changes rather slowly.

Similar behaviour is reported by Albertsson & Elding (1977) for the bromate and ethylsulfate structures, notwithstanding the dissimilarities in the hydrogen-bond arrangements. This behaviour is obviously associated with the differential rate of contraction for the Ln—O(1) and Ln—O(2) bonds. In this respect Albertsson & Elding's (1977) explanation for the phenomenon is also unconvincing. It is difficult to see why steric hindrance with O(2) should weaken the hydrogen-bond system involving O(1). It is more reasonable to associate it with the different bonding arrangements for the ligating oxygens; that is, trigonal for the equatorial oxygens and nearer to tetrahedral for the prism oxygens. The fact that this occurs in all three series of structures indicates that it is a fundamental property of the hydrated metal atom related to the number of metal $4f$ electrons. The electronic properties of the cations affect the packing of the structure *via* their effect on the ligating water molecules.

In the following paper (Chatterjee, Maslen & Watson, 1988) it is shown that the orientation of the water molecules has a pronounced effect on the polarization of the electron density near the metal. Towards the lutetium end of the series the effect of the polarization is repulsive, by an amount which increases with decreasing metal—oxygen distance. The increase is

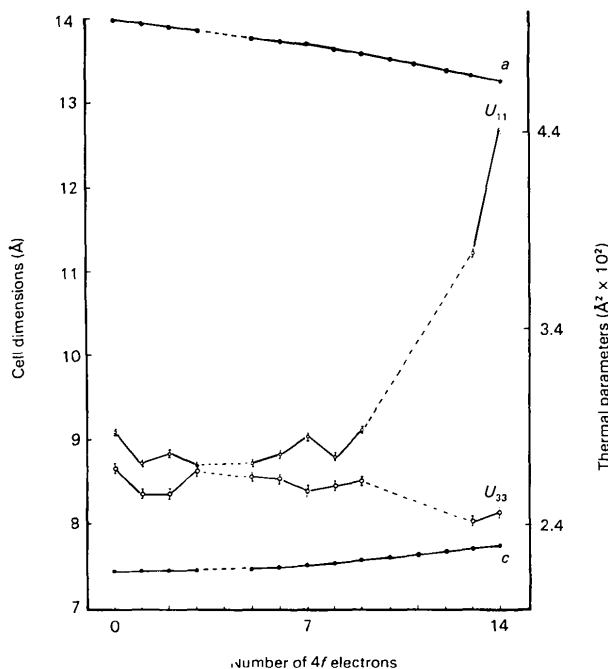


Fig. 1. Unit-cell dimensions and lanthanoid vibration-tensor elements as functions of the number of $4f$ electrons in the corresponding Ln^{III} ion.

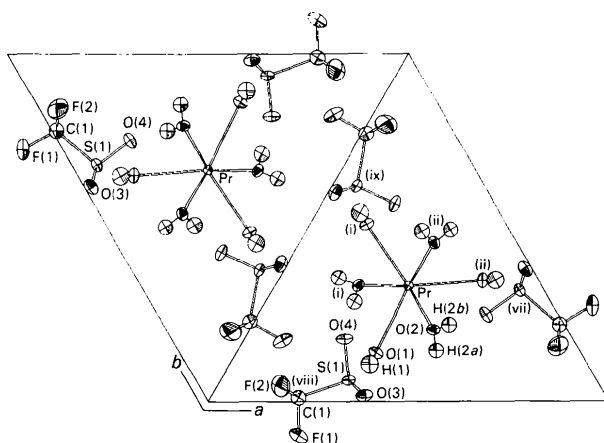


Fig. 2. Representation of the crystal structure of praseodymium triflate, shown as 20% probability ellipsoids, projected on the ab plane. Note the symmetrical (trigonal) geometry about O(1), and the unsymmetrical bonding arrangement about O(2). Symmetry codes are defined in Table 5.

more rapid in the direction of the equatorial oxygens than it is along the vector towards the prism oxygens. This change in the nature of the metal–oxygen interaction with water molecule orientation provides the mechanism for the differential contraction of the bonds to the equatorial and prism waters.

The longer bonds are weaker because there is less overlap between the atomic densities. The weakness of these bonds is reinforced by the repulsive contribution due to polarization of the electron density. This is accompanied by a reduction in strength of the hydrogen bonds linking the ligating waters to the trifluoromethanesulfonate groups, accounting for the tendency for these crystals to lose water at the lutetium end of the series.

All calculations were performed on a Perkin–Elmer 3240 computer using programs from the XRAY76 system (Stewart, 1976). This work was supported financially by the Australian Institute of Nuclear Science and Engineering, and by the Research Committee of the University of Western Australia. One of us (AC) gratefully acknowledges receipt of a University Research Studentship.

References

- ALBERTSSON, J. & ELTING, I. (1977). *Acta Cryst.* B33, 1460–1469.
- BACON, G. E. (1975). *Neutron Diffraction*. Oxford: Clarendon Press.
- CHATTERJEE, A., MASLEN, E. N. & WATSON, K. J. (1988). *Acta Cryst.* B44, 386–395.
- ELCOMBE, M. M., COX, G. W., PRYOR, A. W. & MOORE, F. H. (1971). *Programs for the Management and Processing of Neutron Diffraction Data*. AAEC Report TM578. Australian Atomic Energy Commission, Lucas Heights, New South Wales, Australia.
- FRENCH, S. & WILSON, K. (1978). *Acta Cryst.* A34, 517–525.
- GEIER, G. & KARLEN, U. (1971). *Helv. Chim. Acta*, 54, 135–153.
- GEIER, G., KARLEN, U. & ZELEWSKY, A. V. (1969). *Helv. Chim. Acta*, 52, 1967–1975.
- HARROWFIELD, J. M., KEPERT, D. L., PATRICK, J. M. & WHITE, A. H. (1983). *Aust. J. Chem.* 36, 483–492.
- International Tables for X-ray Crystallography* (1974). Vol. IV. Birmingham: Kynoch Press. (Present distributor Kluwer Academic Publishers, Dordrecht.)
- LARSON, A. C. (1970). *Crystallographic Computing*, edited by F. R. AHMED, pp. 209–213. Copenhagen: Munksgaard.
- MELKONIAN, E. (1949). *Phys. Rev.* 76, 1750–1759.
- MEULENAER, J. DE & TOMPA, H. (1965). *Acta Cryst.* 19, 1014–1018.
- MOORE, F. H. (1981). Private communication.
- PAIVA SANTOS, C. O., CASTELLANO, E. E., MACHADO, L. C. & VICENTINI, G. (1985). *Inorg. Chim. Acta*, 110, 83–85.
- REUBEN, J. & FIAT, D. (1969). *J. Chem. Phys.* 51, 4909–4917.
- SPEDDING, F. H., PIKAL, M. J. & AYRES, B. O. (1966). *J. Phys. Chem.* 70, 2440–2449.
- STEWART, J. M. (1976). The XRAY76 system. Tech. Rep. TR-446. Computer Science Centre, Univ. of Maryland, College Park, Maryland, USA.
- STEWART, R. F., DAVIDSON, E. R. & SIMPSON, W. T. (1965). *J. Chem. Phys.* 42, 3175–3187.

Acta Cryst. (1988). B44, 386–395

Electron Densities in Crystals of Nonaaqualanthanoid(III) Tris(trifluoromethanesulfonates)

BY A. CHATTERJEE, E. N. MASLEN AND K. J. WATSON

Department of Physics, University of Western Australia, Nedlands, Australia 6009

(Received 12 May 1986; accepted 12 February 1988)

Abstract

The deformation electron densities in crystals of the title compounds for Ln = La, Ce, Pr, Nd, Sm, Eu, Gd, Tb, Dy, Yb and Lu were evaluated using X-ray diffraction data measured at room temperature. The deformation density maps for the lanthanum, gadolinium and lutetium complexes are topologically consistent with those of the neighbouring members of the series. That is, the spherical symmetry of the prepared state for the La³⁺, Gd³⁺ and Lu³⁺ ions is not preserved in the bonded complexes. For the lighter members, the deformation densities exhibit a symmetric component with excess electron density near each rare-earth

nucleus which could be associated with a degenerate form of $f-f$ orbital product. This disappears at the lutetium end of the series, consistent with its being forbidden by Fermi–Dirac statistics. Close to all rare-earth nuclei there is a strong tricontadipole deformation density component which increases in magnitude with the number of $4f$ electrons. This feature can be accounted for by a $4f-5d$ contribution to the density. The effect of anharmonicity on the deformation densities is negligible, as indicated by the radial dependence of the principal features, and confirmed by a neutron diffraction experiment for the neodymium complex. Smaller features further from the rare-earth nuclei occur consistently in all maps for the complexes